Journal of Magnetism and Magnetic Materials 587 (2023) 171340

Contents lists available at ScienceDirect

Journal of Magnetism and Magnetic Materials

journal homepage: www.elsevier.com/locate/jmmm

Optimizing power transfer in selective wireless charging systems: A genetic algorithm-based approach

Vittorio Bertolini [a,*], Fabio Corti [b], Matteo Intravaia [b], Alberto Reatti [b], Emiliano Cardelli [a]

[a] University of Perugia, Department of Engineering, Via G. Duranti 93, Perugia 06125, Italy
[b] University of Florence, Department of Information Engineering, Via di Santa Marta 3, Firenze 50139, Italy

ARTICLE INFO

Keywords:
Selective power transfer
Resonant circuits
Genetic algorithms

ABSTRACT

This paper presents a novel approach to optimize selective wireless power transmission to multiple receivers utilizing a single transmitter. The primary focus is on achieving power delivery at specific frequencies, which ensures maximum transmission efficiency. To this end, an analytical model based on magnetic coupling between coils is employed to explore different solutions. Genetic Algorithm (GA) is applied to identify the optimal configuration. The application of GA for system optimization is introduced, which helps effectively dealing with multiple receivers where analytical models become difficult to manage. The GA-based approach facilitates the discovery of various solutions that might be challenging to derive analytically. The validity of the proposed approach is confirmed through simulations and experimental measurements.

1. Introduction

Wireless Power Transfer (WPT) is a technology that enables the transmission of energy from a source to a load without a physical connection. This innovation allows for greater flexibility in the charging process, leading to several advantages [1,2].

The classic structure of a WPT system consists of a primary circuit, where the element operating as a transmitter is located, and a secondary circuit, where the element operating as a receiver is placed. Since the coils are air-coupled, additional components, capacitors and inductors, are usually connected to the primary and secondary circuits, tuned to the operating resonance so that the transmission efficiency is increased. The most widely used topology is the series-series compensation, which allows obtaining high efficiency when operating with low coupling coefficient. For this reason, this topology is referenced throughout the paper.

Recently, Multiple Receiver Wireless Power Transfer (MRWPT), which refers to a technology that enables wireless charging of multiple receivers from a single power transmitter (Fig. 1), has been largely investigated. Several papers are available in the literature focusing on the analysis of the system to optimize the simultaneous charging of multiple devices. For example, in [3], two receivers operating at 100 kHz and 13.56 MHz have been charged simultaneously, delivering 15 W to each load with an efficiency of 82.5% and 74.8% respectively [4]. The different loads have been simultaneously charged with the primary and the secondaries resonant at 145 kHz frequency, transferring a power of 6 W.

In [5], two receivers are simultaneously charged by a single transmitter powered by half-bridge inverter at the same frequency. The receivers resonate at 173 kHz and 206 kHz. Although this solution is extremely basic, it is characterized by high costs, since two inverters connected in parallel are required.

In [6], a selective WPT to multiple receivers tuned at different frequencies is presented. The work proves that the efficiency is maximum when the driving frequency equals the resonant frequency of the receiving coil, regardless of the resonance frequency of the sending one. Anyway, the paper is only focused on transmission efficiency, the power delivered is completely neglected.

In [7], the power is selectively transferred depending on the different resonance frequencies of the receivers and the frequency of the power transmitter. The system operates in the 2–25 MHz frequency range. The resonance frequencies of the receivers differ greatly in order to limit the cross-coupling and power division problem. Anyway, the system works at high frequency where parasitic effects can reduce the efficiency; in fact, the system reached 20% transmission efficiency. Moreover, the large difference

* Corresponding author.
E-mail address: vittorio.bertolini@studenti.unipg.it (V. Bertolini).

https://doi.org/10.1016/j.jmmm.2023.171340
Received 4 August 2023; Received in revised form 27 September 2023; Accepted 1 October 2023
Available online 6 October 2023

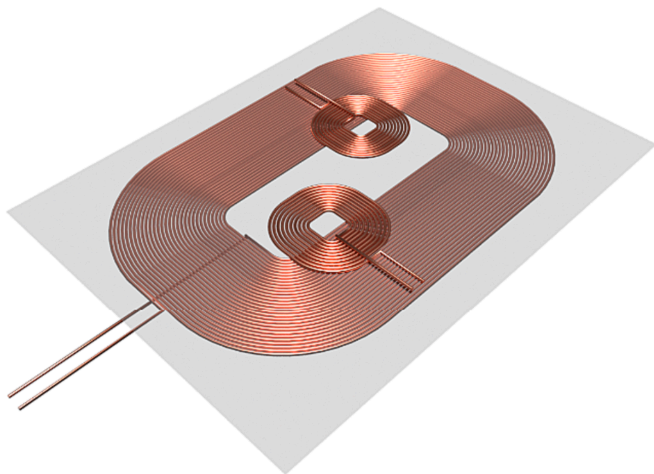

Fig. 1. Illustration of multi-receiver WPT system with two secondaries.

in the receivers of a frequency tuning technique using a variable capacitance in the transmitter to control the difference between the resonance frequency of the transmitter and the selected receiver. In this last case, in fact, a large amount of reactive power would be developed in the transmitter when the receivers work in resonance conditions.

In [8], the power transmitted by an omnidirectional transmitter composed of three orthogonal coils is received by any receiver located around. Based on the band-pass filter principle, the receivers selectively acquire the power at a designated frequency. Anyway, the omnidirectional transmitter is made of three separate coils supplied by an inverter, thus the size and the costs of the system are significant.

This paper focuses on a case of selective power transmission in multiple receivers using a single transmitter. Assuming the characteristics of the receivers are already known (e.g., the resonant frequency), the optimization of the transmitter output to guarantee the achievement of target power on the secondaries and minimum transmission efficiency. An analytical model of the magnetic coupling between the coils is used to investigate the solutions and identify the optimal solution through a Genetic Algorithm (GA).

The main innovative contributions of the paper are:

- The derivation of a procedure for tuning the transmitter to the desired value of output power at the resonance frequency of the transmitter. Unlike many works available in the literature, the proposed solution is not consisting of using a system whose frequency changes according to the load power. Therefore, no additional component (which for other works is proposed, for example in [7,8]) are required, allowing for reducing overall circuit dimensions and costs.
- The utilization of a GA for the system optimization. The proposed approach is particularly useful because the equivalent analytical model is difficult to analyze when the system has many receivers. For this reason, the proposed GA based solution allows finding numerical solutions which are difficult to identify analytically.

This manuscript is organized as follows: in Sect. 2, the equivalent electric model of the multiple-receiver coupled inductors is presented. In Sect. 3, the use of the equivalent model for the GA optimization process is discussed. In Sect. 4, a case study is analyzed through simulation in Matlab-Simulink environment. In Sect. 5, the experimental validation is presented. Finally, in Sect. 6, the conclusions are reported.

2. Electric model of multiple-receiver wireless power transfer system

The scheme of the WPT system, consisting in a transmitter and two receivers, is shown in Fig. 2. A square wave input voltage $v_i(t)$ is provided to the system. L_1, L_2 and L_3 are the self-inductance coefficients, respectively, of the transmitter and receiver coils. C_1, C_2 and C_3 are the capacitance values of the capacitors inserted in the respective inductors to reach the resonance condition for a specific working frequency; r_1, r_2 and r_3 are the equivalent series resistances (ESRs) associated to each of the LC series connection.

Finally, R_2 and R_3 are the load resistances of the receivers. Applying the KVL (Kirchhoff Voltage Law) to the three loops, the following equations in time domain are derived:

$$L_1\frac{di_1}{dt}+V_{c1}+M_{12}\frac{di_2}{dt}+M_{13}\frac{di_3}{dt}+r_1i_1=v_i \quad (1)$$

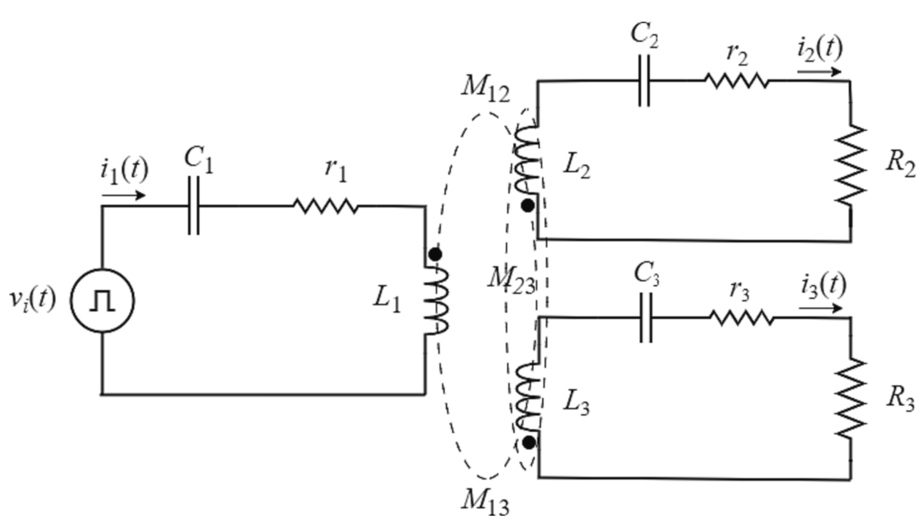

Fig. 2. Two-receiver WPT system.

$$L_2\frac{di_2}{dt}+V_{c2}+M_{21}\frac{di_1}{dt}+M_{23}\frac{di_3}{dt}+(R_2+r_2)i_2=0 \quad (2)$$

$$L_3\frac{di_3}{dt}+V_{c3}+M_{31}\frac{di_1}{dt}+M_{32}\frac{di_2}{dt}+(R_3+r_3)i_3=0 \quad (3)$$

where the mutual inductance coefficients are defined as follows:

$$M_{12}=M_{21}=k_{12}\sqrt{L_1L_2} \quad (4)$$

$$M_{13}=M_{31}=k_{13}\sqrt{L_1L_3} \quad (5)$$

$$M_{23}=M_{32}=k_{23}\sqrt{L_2L_3} \quad (6)$$

k_{12}, k_{13}, k_{23} are the coupling coefficients among the coil 1 (transmitter), 2 (1st receiver) and 3 (2nd receiver). Manipulating Eqs. (1)–(3), the system can be written in matrix form as follows:

$$\begin{bmatrix} L_1 & M_{12} & M_{13} \\ M_{21} & L_2 & M_{23} \\ M_{31} & M_{32} & L_3 \end{bmatrix}\frac{d^2\boldsymbol{i}}{dt^2}+\begin{bmatrix} r_1 & 0 & 0 \\ 0 & R_2+r_2 & 0 \\ 0 & 0 & R_3+r_3 \end{bmatrix}\frac{d\boldsymbol{i}}{dt}+\begin{bmatrix} {}^1/_{C_1} & 0 & 0 \\ 0 & {}^1/_{C_2} & 0 \\ 0 & 0 & {}^1/_{C_3} \end{bmatrix}\boldsymbol{i}=\boldsymbol{u} \quad (7)$$

where $\boldsymbol{i}=[i_1\ i_2\ i_3]^T$ and $\boldsymbol{u}=\left[\frac{dv}{dt}\ 0\ 0\right]^T$.

Note that system (7) can be easily generalized for a WPT system with n receivers, as shown in Fig. 3. System (7) can be extended as follows:

$$\begin{bmatrix} L_1 & M_{12} & M_{13} & \cdots & M_{1n} & M_{1(n+1)} \\ M_{21} & L_2 & M_{23} & \cdots & M_{2n} & M_{2(n+1)} \\ M_{31} & M_{32} & L_3 & \cdots & M_{3n} & M_{3(n+1)} \\ \vdots & \vdots & \vdots & \cdots & \vdots & \vdots \\ M_{n1} & M_{n2} & M_{n3} & \cdots & L_n & M_{n(n+1)} \\ M_{(n+1)1} & M_{(n+1)2} & M_{(n+1)3} & \cdots & M_{(n+1)n} & L_{n+1} \end{bmatrix}\frac{d^2\boldsymbol{i}}{dt^2}+\begin{bmatrix} r_1 & 0 & 0 & \cdots & 0 & 0 \\ 0 & (R_2+r_2) & 0 & \cdots & 0 & 0 \\ 0 & 0 & (R_3+r_3) & \cdots & 0 & 0 \\ \vdots & \vdots & \vdots & \cdots & \vdots & \vdots \\ 0 & 0 & 0 & \cdots & (R_n+r_n) & 0 \\ 0 & 0 & 0 & \cdots & 0 & (R_{n+1}+r_{n+1}) \end{bmatrix}\frac{d\boldsymbol{i}}{dt}+\begin{bmatrix} 1/C_1 & 0 & 0 & \cdots & 0 & 0 \\ 0 & 1/C_2 & 0 & \cdots & 0 & 0 \\ 0 & 0 & 1/C_3 & \cdots & 0 & 0 \\ \vdots & \vdots & \vdots & \vdots & \vdots & \vdots \\ 0 & 0 & 0 & \cdots & 1/C_n & 0 \\ 0 & 0 & 0 & \cdots & 0 & 1/C_{n+1} \end{bmatrix}\boldsymbol{i}=\boldsymbol{u} \quad (8)$$

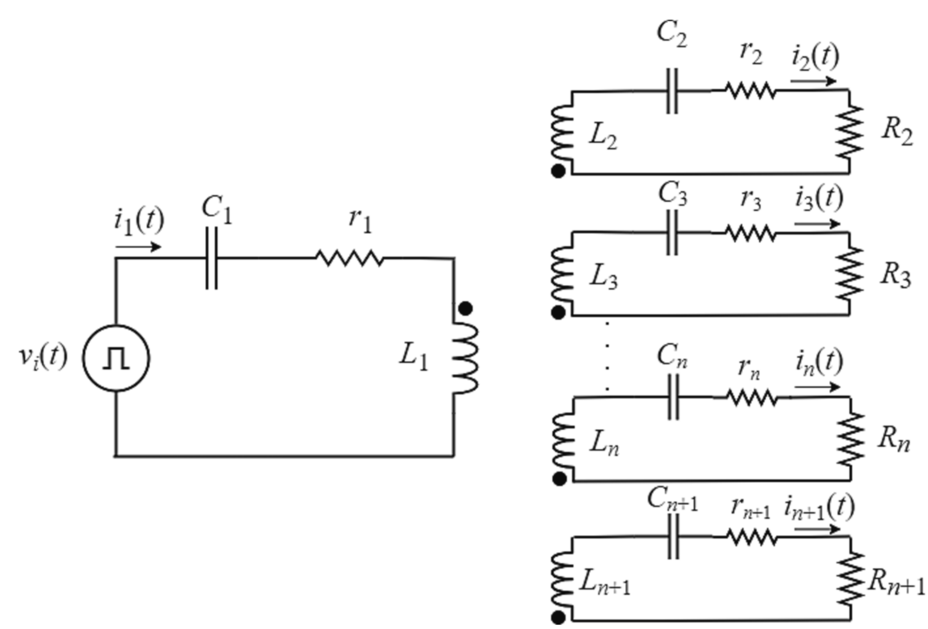

Fig. 3. N-receivers WPT system.

When the working frequency of the transmitter is the resonant frequency of the receivers and is far from the LC-C poles, the receivers behave like band-pass filters, so that the harmonics provided by the square wave input voltage are suppressed, with the exception of the fundamental one. On the other hand, the transmitter, which does not achieve resonance conditions, is crossed by a periodic non-harmonic current; however, it is very low, because it is damped by the non-resonant impedance and the charge mechanism of the resonant coil. Consequently, the system can be studied considering the first harmonic of the square wave input voltage, since the contribution of the other harmonics is considered negligible. In this way, the system expressed in (7) can be written in the frequency domain using a phasor approach, which is an easy way to describe the steady-state behavior of the system. The equation system (9) is obtained with all the variables defined above.

$$\begin{bmatrix} j\omega L_1 - \dfrac{j}{\omega C_1} + r_1 & j\omega M_{12} & j\omega M_{13} \\ j\omega M_{21} & j\omega L_2 - \dfrac{j}{\omega C_2} + r_2 & j\omega M_{23} \\ j\omega M_{31} & j\omega M_{32} & j\omega L_3 - \dfrac{j}{\omega C_3} + r_3 \end{bmatrix} \dot{\mathbf{I}} = \dot{\mathbf{U}} \quad (9)$$

where $\dot{\mathbf{I}} = \left[\dot{I}_1\ \dot{I}_2\ \dot{I}_3\right]^T$ and $\dot{\mathbf{U}} = \left[\dot{V}_i\ 0\ 0\right]^T$. From (9), the phasors of the currents flowing in the transmitter and the receivers are expressed as:

$$\dot{\mathbf{I}} = \begin{bmatrix} j\omega L_1 - \dfrac{j}{\omega C_1} + r_1 & j\omega M_{12} & j\omega M_{13} \\ j\omega M_{21} & j\omega L_2 - \dfrac{j}{\omega C_2} + (R_2 + r_2) & j\omega M_{23} \\ j\omega M_{31} & j\omega M_{32} & j\omega L_3 - \dfrac{j}{\omega C_3} + (R_3 + r_3) \end{bmatrix}^{-1} \dot{\mathbf{U}} \quad (10)$$

Once the currents are determined, the power delivered to the loads and the efficiency of the power transmission to each load can be calculated:

$$P_{r1} = R_2|I_2|^2,\ P_{r2} = R_3|I_3|^2 \quad (11)$$

$$\eta_{r1} = \frac{R_2|I_2|^2}{r_1|I_1|^2 + (R_2 + r_2)|I_2|^2 + (R_3 + r_3)|I_3|^2} \quad (12)$$

$$\eta_{r2} = \frac{R_3|I_3|^2}{r_1|I_1|^2 + (R_2 + r_2)|I_2|^2 + (R_3 + r_3)|I_3|^2} \quad (13)$$

Eqs. (9)-(13) are a generalization for the receivers of the system expressed in (8) written in the frequency domain.

3. Genetic algorithm optimization

GAs are powerful optimization techniques inspired by the principle of Darwinian evolution theory. The algorithm employs mechanisms such as crossover, mutation, and natural selection to identify the fittest individuals for a specific condition. This process is responsible for finding the optimal solution that minimizes or maximizes the objective function, commonly referred to as the fitness function. GAs have been noticed to be a valid alternative to other strategies, especially in highly multi-parameter multi-objective problems. Additionally, GAs explore the parameter space extensively via a random generation of a diverse initial population, thereby avoiding local optima and finding the global optimal solution [9]. As such, GAs appear to be effective when dealing with circuit design problems, such as the determination of multi-coil components, which typically have a large search space and multiple requirements [10,11].

Generally, a single-objective GA workflow involves the following steps:

1. Problem formulation: definition of the optimization parameters (the genes of the individuals), the parameter constraints and the fitness function.
2. First generation: first set of individuals generated by randomly selecting the genes inside the provided constraints.
3. Fitness calculation: the fitness function is computed for each individual.
4. Selection: the fittest individuals of the population are identified.
5. Crossover: a new generation is created by combining the genes of the previous best individuals (the fittest ones), individuated at step 4, that have better chances to reproduce; therefore, their genes have better chances to be inherited.
6. Mutation: genes of the new generation are slightly altered randomly. This step emulates the natural mutation mechanism, allowing the evolution of the population.
7. Steps 3 to 6 are repeated until a certain criterion is met (e.g., maximum number of generations, fitness function value).
8. Results: the fittest individuals of the last generation represent the optimization results.

Fig. 4 recaps this procedure with a flowchart.

In multi-objective optimization, there is more than one fitness function at the same time; the algorithm structure is the same, but the fitness evaluation becomes more complicated, the fitness function has multiple components, one for each objective; the algorithm has to identify the so-called Pareto front, which is the locus of the solutions, in the parameter space, where no objective can be improved without worsening other objectives. The solutions lying on the Pareto front are called "non-dominated" solutions.

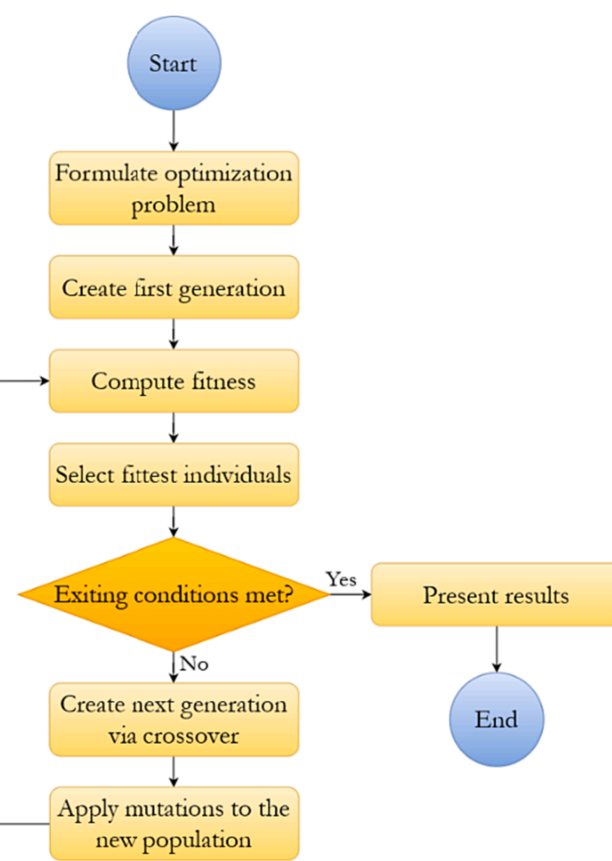

Fig. 4. Typical single-objective GA flowchart.

The algorithm adopted in this work is a Non-dominated Sorting Genetic Algorithm (NSGA-II) [12], implemented in Matlab. It is based on the concept of ranking individuals at each generation: non-dominated solutions are assigned to rank one; individuals dominated only by rank one solutions are assigned to rank two, and so on. Going through the generations, the solutions move toward the actual Pareto front.

A. Optimization problem formulation

The implemented NSGA-II algorithm optimizes the primary circuit parameters to transfer selectively the power to the receivers while keeping the efficiency as high as possible. A two-receiver MPT system is examined as a case study, but the method can be easily extended to n-receiver WPT systems exploiting the equation (8). The optimization problem for the two-receiver configuration consists of six fitness functions, depending on five parameters (genes). The problem formulation is the following:

$$\underset{x}{\text{minimize}}\ f_i(x), \quad i = 1, \cdots, 6$$

Subject to

$$L_j < x_j < U_j \tag{14}$$

where f_i is the i-th fitness function, x is the vector containing the genes, L_j and U_j are respectively the lower and the upper bound for the j-th gene value x_j. The genes with the respective lower and upper bounds are listed in Table 1.

The fitness functions are expressed as follows:

$$ff_1 = \left[P_{r1}|_{f_1} - P_{obj1}\right]^2 \tag{15}$$

$$ff_2 = \left[P_{r2}|_{f_2} - P_{obj2}\right]^2 \tag{16}$$

$$ff_3 = P_{r1}|_{f_2} \tag{17}$$

$$ff_4 = P_{r2}|_{f_1} \tag{18}$$

$$ff_5 = 1 - \eta_{r1}|_{f_1} \tag{19}$$

$$ff_6 = 1 - \eta_{r2}|_{f_2} \tag{20}$$

where $P_r|_{f_j}$ is the power on the load of the receiver r calculated at the working frequency f_j, P_{obj_i} is the objective output power for the i-th receiver, $\eta_r|_{f_j}$ is the power transmission efficiency of the receiver r calculated at the working frequency f_j. The power on the receiver loads and the efficiencies are computed using equations (10)–(13). Essentially, (15) and (16) express the intention to output the power on each receiver approaching the objective power when working at the appropriate frequency (i.e., f_1 for receiver 1, f_2 for receiver 2); (17) and (18) try to realize the selectivity of the WPT system, minimizing the power transferred when working at the "wrong" frequency (f_2 for receiver 1, f_1 for receiver 2); finally, (19) and (20) try to maximize the power transmission efficiency.

Table 1
Genetic algorithm genes with the respective lower and upper bounds.

Gene	Description	Lower bounds L_j	Upper bounds U_j
V_{in}^{rms}	Input voltage RMS value	20 V	80 V
L_1	Transmitter inductance	1 μH	100 μH
C_1	Transmitter capacitance	1 μF	100 μF
f_1	Working frequency of the 1st receiver	5 kHz	500 kHz
f_2	Working frequency of the 2nd receiver	5 kHz	500 kHz

Table 2
System parameters in the example case study.

Parameter	Assigned value	Description
r_1	0.1 Ω	Primary parasitic resistance
L_2	2.8 μH	Receiver 1 inductance
C_2	33 nF	Receiver 1 capacitance
R_2	10 Ω	Receiver 1 load
r_2	0.05 Ω	Receiver 1 parasitic resistance
L_3	1.8 μH	Receiver 2 inductance
C_3	1.65 nF	Receiver 2 capacitance
R_3	1 Ω	Receiver 2 load
r_3	0.05 Ω	Receiver 2 parasitic resistance
k_{12}	0.34	Coupling coefficient between primary and receiver 1 coils
k_{13}	0.11	Coupling coefficient between primary and receiver 2 coils
k_{23}	0.01	Coupling coefficient between the two receiver coils

A case study is established by fixing the system parameters (excluded the parameters to be optimized) in Table 2. These values are used to solve the optimization problem, leaving out the parameters of Table 1 (see Section 3B). Section 3B also provides details concerning GA setting and execution. The results are compared with the WPT system measurements, which is subsequently simulated and experimentally verified, presented in Section 4 and Section 5, respectively.

B. Optimization results

The adopted NSGA-II selects randomly the initial population within the respective bounds. Each subsequent generation is created for 80% via crossover and 20% by randomly selecting genes within the specified bounds. Mutation is applied to each individual by perturbing it in a random direction in the parameter space, then the fitness of the perturbed point is checked with respect to the previous generation, so that the solution is mutated if the fitness gets better. The computation time is around 4 hours, with a small variation of about 0.5 h due to the starting values of the genes and to the random mutation. The solution convergence requires from 100 to 200 generations; the number of fitness function evaluations is between 5000 and 10000.

Using the parameters in Table 2, we performed hundreds of optimizations. For each, the NSGA-II results in optimized solutions on the Pareto front; the solution individuated is the one closest to the origin in the objective space, i.e., the solution having the minimum sum of the fitness function values. At the end of this process, over all the results, a single solution has been selected (see Table 3), which is used in the following simulations and experiments. Computing the output power on the two receivers and the efficiency with respect to frequency, by exploiting the equations presented in Section 2, and using the parameters provided in Table 3, the curves shown in Fig. 5 are obtained. The target output power is reached with an excellent accuracy for the receivers when working at f_1 and f_2 frequencies, respectively for receiver 1 and receiver 2. The transmission efficiency is over 80% in both the cases. Additionally, notice that, when working at frequency f_1, the power leaking to the second receiver is almost null; conversely, when working at frequency f_2, a small amount of energy is transferred to the first receiver,

Table 3
Final optimized values for experimentation.

Gene	Solution (optimized values) for experimentation
V_{in}^{rms}	62.5 V
L_1	9.3 μH
C_1	5.5 μF
f_1	19.2 kHz
f_2	29.6 kHz

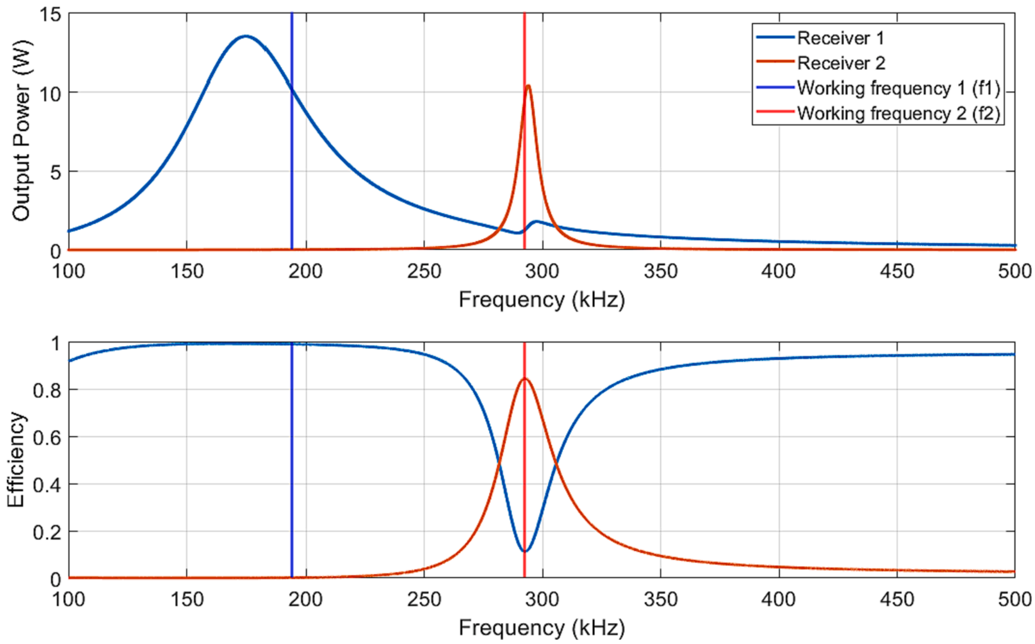

Fig. 5. Output power and efficiency of the system depending on the frequency of two receivers using the optimized solution in Table 3. The working frequencies are individually chosen by the GA and are aligned with the colored vertical lines.

Table 4
Performance (deviation from objectives) of the solution in Table 3.

Fitness function	Objective	Error (deviation from objective)	Description
f_1	10 W	0.2 W	Output power on receiver 1 at frequency f_1
f_2	10 W	0.3 W	Output power on receiver 2 at frequency f_2
f_3	0 W	1.3 W	Output power on receiver 1 at frequency f_2
f_4	0 W	0.015 W	Output power on receiver 2 at frequency f_1
f_5	1	0.02	Transfer efficiency receiver 1 at frequency f_1
f_6	1	0.16	Transfer efficiency receiver 2 at frequency f_2

making the WPT system electrically perfect. This aspect is reflected both in the simulation and in the experiments (see Sections 4 and 5). Table 4 recaps the performance of the algorithm, in terms of deviation from the objectives, of the solution of Table 3.

4. Simulation results

The system has been evaluated in a Simulink environment. The simulation is performed in the time domain applying a sinewave input voltage. Therefore, the simulation results correspond well with the behavior of the real system. In the results predicted by the analytical model have been obtained considering sinusoidal input voltages, as stated in Section 2, which is reliable only if the system works in resonant condition. The resonant frequencies of the two receivers are evaluated by analyzing the phase of the currents through the secondary circuits using the model presented in Section 2 with the parameters in Table 2 and Table 3, the current phases of the two receivers for different working frequencies are evaluated. The results are shown in Fig. 6.

The resonant condition occurs when the current phase shifts from negative to positive values (or vice versa), since the overall circuit impedance changes sign at resonance. According to Fig. 6, the resonant

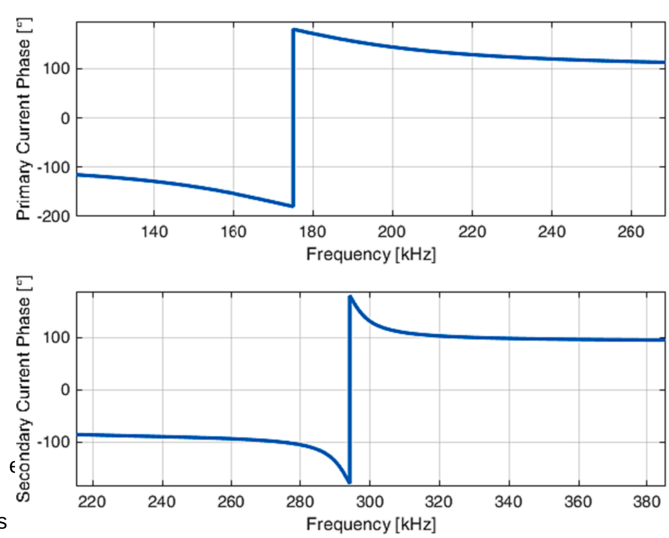

Fig. 6. Current phases of the receivers for different working frequencies.

frequencies of the two receivers are, respectively, 175 kHz and 294 kHz. So, the system works at frequencies far from the resonances (typically about ±20% of the resonant frequency). In this case, the working frequencies to obtain 10 W in the receivers respect the hypothesis. For this reason, the simulation is expected to be similar to the predicted one by the analytical model. In Fig. 7, the voltages across the two resistors R_2 and R_3 are shown for two working frequencies 192 kHz (Fig. 7a) and 292 kHz (Fig. 7b), respectively. When the system works at f_1 = 192 kHz, the first receiver is at its resonant condition, thus it can be seen how the voltage on R_2 is almost a pure sinusoid, while the voltage on R_3 is distorted. The mean output power (evaluated in the time domain) is 10.7 W on R_2 and 0.015 W on R_3. Different is the case of f_2 = 292 kHz, where the voltage on R_2 is distorted while the voltage on R_3 is sinusoidal. The peak voltages are similar since the resistors are different ($R_2 = 10R_3$), the current flowing in R_2 is almost ten times smaller than the one flowing in R_3. The mean

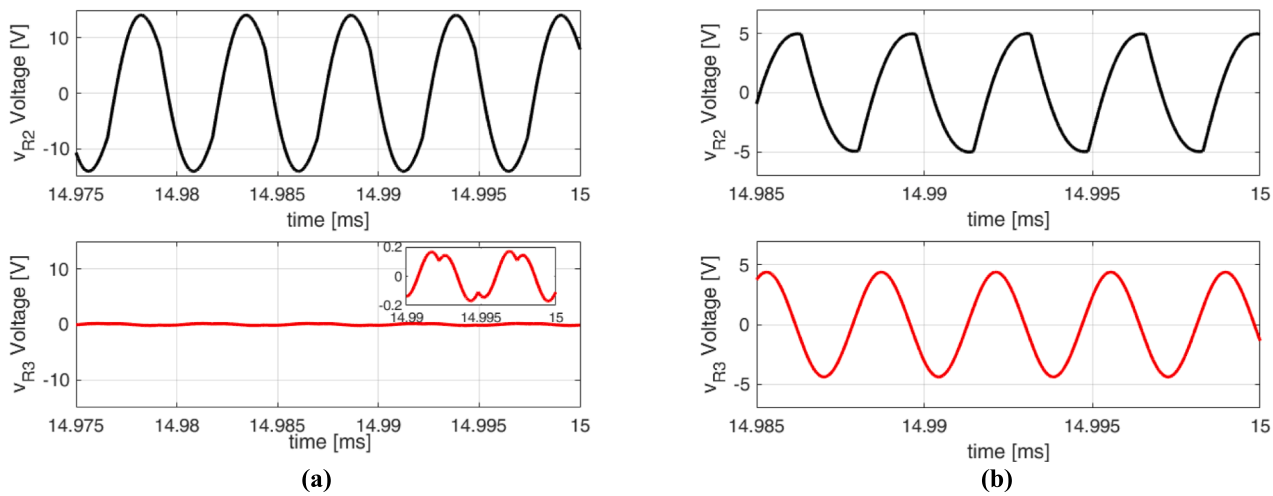

Fig. 7. Voltages across the resistors for f = 192 kHz (a) and f = 292 kHz (b).

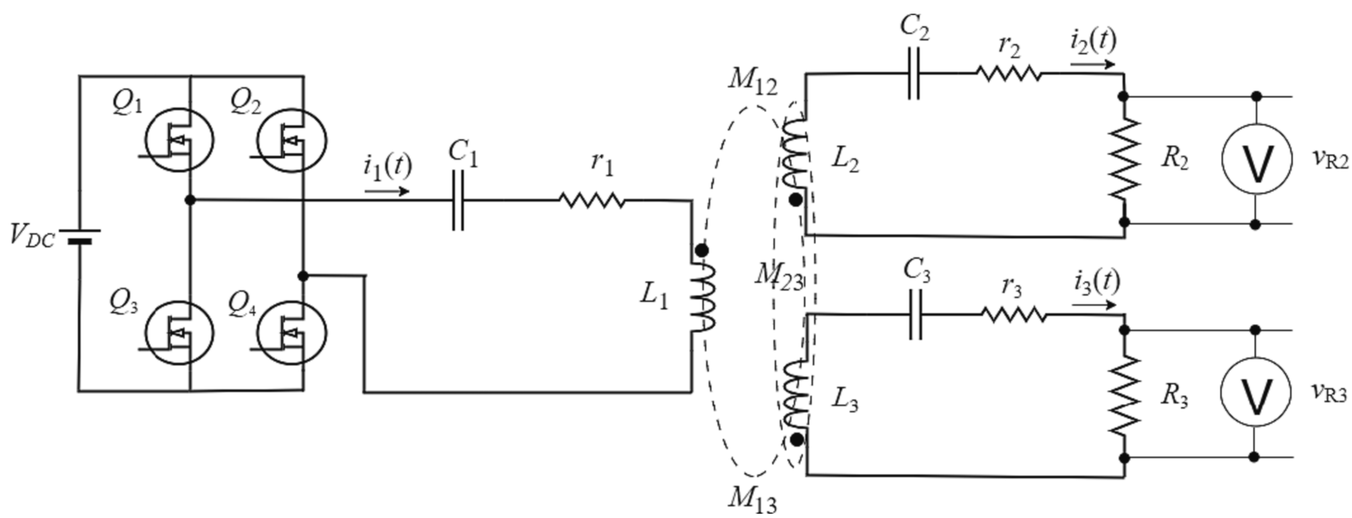

Fig. 8. Schematic of the WPT system.

power in R_2 is equal to 1.58 W, while the power in R_3 is 1.27 W. In both cases, as expected, the simulated energy is in accordance with the results predicted by the analytical model. In particular, it can be seen how selecting the working frequency, one can select the receiver which receives most of the available power.

5. Experimental validation

To experimentally validate the analytical results obtained in the previous sections, the electric circuit shown in Fig. 8 has been realized. It consists of a self-built inverter connected to a voltage generator source V_{DC}. The three transmitting and receiving coils have been realized using Litz wire (to minimize the skin effect) with equivalent AWG 3 (American Wire Gauge) made up by 12,640 strands of AWG 38. The inductances and the Equivalent Series Resistances (ESR), measured at 200 kHz, are shown and compared with the analytical ones in Table 5.

Table 5
Calculated and measured inductances.

Parameter	Analytical	Measured
L_1	9.3 μH	9.13 μH / ESR_1 = 33.4 mΩ
L_2	2.8 μH	2.69 μH / ESR_2 = 27.9 mΩ
L_3	1.8 μH	1.89 μH / ESR_3 = 15.2 mΩ

Table 6
Calculated and measured capacitances.

Parameter	Analytical	Measured
C_1	5.5 μF	1× EZPE50107MTA 5.62 μF / ESR_1 = 22.1 mΩ
C_2	3.3 nF	1× FKP1T023306D00JSSD 3.39 nF / ESR_2 = 23.4 mΩ
C_3	1.65 nF	2× FKP1T023306D00JSSD (in series) 1.58 nF / ESR_3 = 43.6 mΩ

For the three resonance capacitors shown in Table 2 and Table 3, the connections in series/parallel of capacitors shown in Table 6 have been used.

The experimental setup shown in Fig. 9 has been arranged to reproduce the circuit in Fig. 8. The values of the capacitances and the inductances have been measured using a LCR 400 meter by Thurlby Thandar Instruments. The voltages and currents waveforms have been measured using a RTM3004 oscilloscope at 5 GSa/s

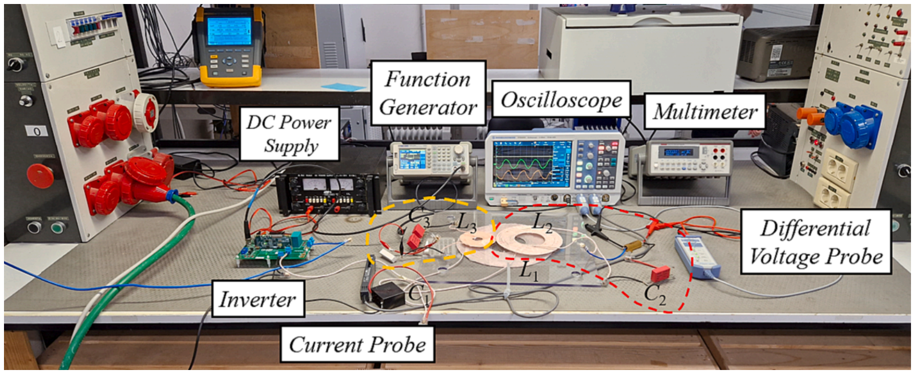

Fig. 9. Experimental setup.

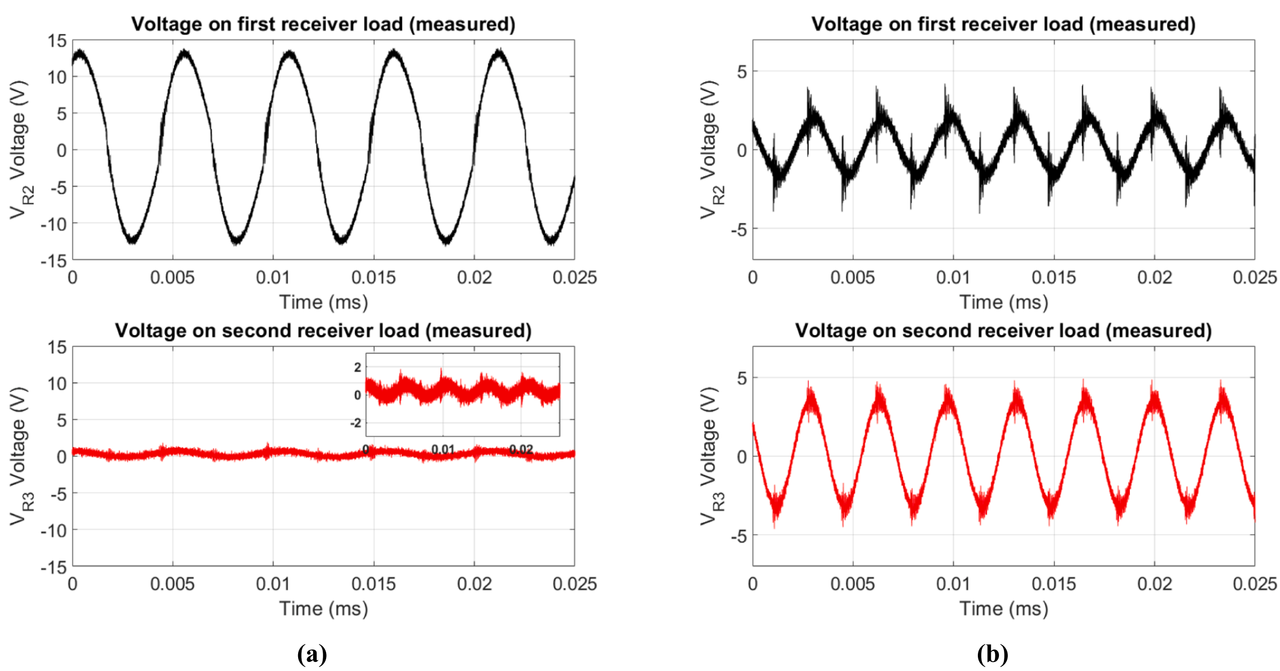

Fig. 10. Voltages across the load resistances measured experimentally: (a) $f_1 = 192$ kHz; (b) $f_2 = 292$ kHz.

Table 7
Comparison between analytical and experimental output power.

Operating Condition	Output Power Delivered to R_2		Output Power Delivered to R_3	
	Analytical	Experimental	Analytical	Experimental
$f_1 = 192$ kHz	10.7 W	9.94 W	0.015 W	0.05 W
$f_2 = 292$ kHz	0.45 W	0.48 W	9.58 W	8.91 W

Rhode & Schwarz AG. GaN Systems GS66508T-EVBDB2 board has been used as half-bridge inverter.

The two receivers have been suitably placed to obtain the coupling coefficients $k_{12} = 0.13$ and $k_{13} = 0.11$.

The primary inverter is operated with a square wave voltage with duty cycle $D = 0.5$ and DC voltage $V_{DC} = 63$ V. The frequency has been changed to evaluate the validity of the analytical model.

In Fig. 10 the voltage across R_2 (black trace) and the voltage across R_3 (red trace) are shown.

In Fig. 10(a) the case when the inverter operates at $f_1 = 192$ kHz is shown. The peak amplitude of the measured output voltage on R_2 is $V_{R2} = 14.1$ V (black curve), while the voltage across R_3 hardly reaches 1 V (red trace). The experimental results of the performance of the proposed selective power transfer to the load R_2 is $P_O^{R2} = 9.94$ W, while the transferred power to the load R_3 is $P_O^{R3} = 0.05$ W, as shown in Table 7.

In Fig. 10(b) the case when the inverter operates at $f_2 = 292$ kHz is shown. The amplitude of the measured output voltage on R_3 is $V_{R2} = 3.1$ V (black curve), while the voltage across R_3 is $V_{R3} = 4.2$ V (red trace). The experimental results of the performance of the proposed selective power transfer to R_3 is $P_O^{R3} = 8.91$ W while the transferred power to the load R_2 is $P_O^{R2} = 0.48$ W, as shown in Table 7.

6. Conclusions

This paper presents a new design procedure for selective WPT system. The analysis is extended to a system with several receivers characterized by different resonant frequencies. The design process is based on the proper selection of the transmitter capacitance (that act as a notch) to allow a selective power transmission to the receivers at different frequencies. The proposed solution uses a GA to identify the most suitable component values of the primary system. The proposed approach significantly by its simplicity and extendibility to other cases where more currents or more coils are involved, which would make the use of analytical approaches difficult. Since the problem presented in this work features multiple functions directly in conflict with each other, NSGA-II is able to find optimal configurations for complex problems like this, likely avoiding local minima. As a further study, the problem formulation can be enhanced, including for instance effects such as the skin effect in conductors; the fitness function topology may get more complex, with the appearance of local minima where the GA can get stuck. In these cases, the application of some more advanced multi-objective algorithms (such as the Strength Pareto Evolutionary Algorithm 2, Multi-Objective Particle Swarm Optimization, Multi-Objective Artificial Bee Colony, Non-dominated Sorting Particle Swarm Optimization) can be helpful in finding the ideal approach to reach the global optimum.

The accuracy of the proposed approach is experimentally validated, and experimental results match the theoretically expected data.

Declaration of Competing Interest

The authors declare that they have no known competing financial interests or personal relationships that could have appeared to influence the work reported in this paper.

Data availability

Data will be made available on request.

References

[1] C.H. Lee, G. Jung, K.A. Hosani, B. Song, D.-K. Seo, D. Cho, Wireless Power Transfer System for an Autonomous Electric Vehicle, in: 2020 IEEE Wireless Power Transfer Conference (WPTC), Seoul, Korea (South), 2020, pp. 467–470, doi: 10.1109/WPTC48563.2020.9295631.

[2] F. Tavernier, R. Scorretti, N. Burais, H. Razik, Y. Gaspard, Real-Time Numerical Dosimetry of Low-Frequency Electromagnetic Fields by Using Multi-GPUs, IEEE Trans. Magn. 57 (6) (Jun. 2021) 1–4, Art no. 9001004, doi: 10.1109/TMAG.2021.3065554.

[3] M. Liu, M. Chen, Dual-Band Wireless Power Transfer With Reactance Steering Network and Reconfigurable Receivers, IEEE Trans. Power Electron. 35 (1) (Jan. 2020) 496–507, https://doi.org/10.1109/TPEL.2019.2

[4] Q.-V. Tran, Q.-D. Tuong, M. Okada, Load-Independent Voltage Output from Multiple-Receiver Inductive Power Transfer Systems, IEEE Access 7 (2019) 39453–39461, https://doi.org/10.1109/ACCESS.2019.2943541

[5] Y. Huang, C. Liu, Y. Xiao, S. Liu, Separate Power Allocation and Control Method Based on Multiple Power Channels for Wireless Power Transfer, IEEE Trans. Power Electron. 35 (9) (Sep. 2020) 9046–9056, https://doi.org/10.1109/TPEL.2020.2973465

[6] Y. Zhang, T. Lu, Z. Zhao, F. He, K. Chen, L. Yuan, Selective Wireless Power Transfer to Multiple Loads Using Receivers of Different Resonant Frequencies, IEEE Trans. Power Electron. 30 (11) (Nov. 2015) 6001–6005, https://doi.org/10.1 TPEL.2014.2347966

[7] Y.-K. Jin, D. Ha, W.J. Chappell, P.P. Irazoqui, Selective Wireless Power Transfer for Smart Power Distribution in a Miniature-Sized Multiple-Receiver System, IEEE Trans. Ind. Electron. 63 (3) (March 2016) 1853–1862, https://doi.org/10 TIE.2015.2493142

[8] Z. Dai, Z. Fang, H. Huang, Y. He, J. Wang, Selective Omnidirectional Magnetic Resonant Coupling Wireless Power Transfer With Multiple-Receiver System, IEEE Access 6 (2018) 19287–19294, https://doi.org/10.1109/ACCES

[9] Y.-W. Leung, Y. Wang, Multiobjective programming using uniform design and genetic algorithm, IEEE Trans. Syst. Man Cybern. Part C (Appl. Rev.) 30 (3) (Aug. 2000) 293–304, https://doi.org/10.1109 5326.885111

[10] A. El Beqal, B. Benhala, I. Zorkani, A Genetic algorithm for the optimal design of a multistage amplifier, International Journal of Electrical and Computer Engineering (IJECE), http://doi.org/10.11591/ijece.v

[11] S.S. Mostafa, N. Horta, A.G. Ravelo-García, F. Morgado-Dias, Analog active filter design using a multi objective genetic algorithm, AEU - International Journal of Electronics and Communications, Volume 93, September 2018, Pages 83–94, https://doi.org/10.1016/j.aeue.2018.06.001.

[12] K. Deb, S. Agrawal, A. Pratap, T. Meyarivan, A fast elitist non-dominated sorting genetic algorithm for multi-objective optimization: NSGA-II, in: Parallel Problem Solving from Nature PPSN VI: 6th International Conference, Paris, France, September 18–20, 2000 Proceedings 6, Springer Berlin Heidelberg, 2000,